



# Simulation of GR19 sodium boiling experiments with cathare 2 system code and Trio\_U MC subchannel code

M. Anderhuber, A. Gerschenfeld, N. Alpy, J. Perez, J.-M. Seiler

## ► To cite this version:

M. Anderhuber, A. Gerschenfeld, N. Alpy, J. Perez, J.-M. Seiler. Simulation of GR19 sodium boiling experiments with cathare 2 system code and Trio\_U MC subchannel code. NURETH-16 - 16th International Topical Meeting on Nuclear Reactor Thermal Hydraulics, Aug 2015, Chicago, United States. cea-02509177

**HAL Id: cea-02509177**

**<https://cea.hal.science/cea-02509177>**

Submitted on 16 Mar 2020

**HAL** is a multi-disciplinary open access archive for the deposit and dissemination of scientific research documents, whether they are published or not. The documents may come from teaching and research institutions in France or abroad, or from public or private research centers.

L'archive ouverte pluridisciplinaire **HAL**, est destinée au dépôt et à la diffusion de documents scientifiques de niveau recherche, publiés ou non, émanant des établissements d'enseignement et de recherche français ou étrangers, des laboratoires publics ou privés.

# **SIMULATION OF GR19 SODIUM BOILING EXPERIMENTS WITH CATHARE 2 SYSTEM CODE AND TRIO\_U MC SUBCHANNEL CODE**

**M. Anderhuber and A. Gerschenfeld**

Commissariat à l'Energie Atomique et aux Energies Alternatives, CEA  
Département de Modélisation des Systèmes et Structures, 91191 Gif-sur-Yvette, France  
[marine.anderhuber@cea.fr](mailto:marine.anderhuber@cea.fr), [antoine.gerschenfeld@cea.fr](mailto:antoine.gerschenfeld@cea.fr),

**N. Alpy and J. Perez**

Commissariat à l'Energie Atomique et aux Energies Alternatives, CEA  
Département d'Etudes des Réacteurs, 13108 Saint-Paul-Lez-Durance, France  
[nicolas.alpy@cea.fr](mailto:nicolas.alpy@cea.fr), [jorge.perezmanes@cea.fr](mailto:jorge.perezmanes@cea.fr)

**JM. Seiler**

Commissariat à l'Energie Atomique et aux Energies Alternatives, CEA  
Département de Technologie Nucléaire, 38000 Grenoble, France  
[jean-marie.seiler@cea.fr](mailto:jean-marie.seiler@cea.fr)

## **ABSTRACT**

The CEA R&D program on SFRs includes the study of reactor behavior during accidental transients possibly leading to sodium boiling, such as an unprotected loss of flow. To that end, two existing CEA thermal hydraulic codes are being extended to model two-phase sodium flows: CATHARE (system dynamics) and Trio\_U MC (subchannel). In the case of the 6-equations CATHARE code, the applicability of its current closure laws to two-phase sodium flow must be evaluated; for the 3-equations MC code, new numerical methods are needed as well.

This paper reports simulations with these codes of the GR19 sodium boiling experiments done at CEA Grenoble in the 80's. Simulations of boiling test on this 19-pin out-of-pile mock-up were undertaken in order to provide a preliminary validation of the two codes and to guide future code improvements.

The results presented here show that CATHARE can achieve good agreement with the experimental data: however, some closure laws (especially for heat transfer) will still have to be revised to better fit sodium boiling physics. Meanwhile, Trio\_U MC is capable of predicting correctly the occurrence and extension of local boiling in boiling steady states: however, further improvements will be needed to correctly model unstable and transient boiling.

## **KEYWORDS**

CATHARE, Trio\_U MC, SFR, sodium boiling, GR19 experiment

## **1. INTRODUCTION**

Sodium Fast Reactors (SFRs) exhibit a large margin to coolant boiling under nominal operating conditions : the typical SFR core outlet temperature averages 550°C (with a maximum fluid temperature around 610°C), while the sodium saturation temperature at atmospheric pressure is around 880°C (and is closer to 920°C in reactor conditions). Nevertheless, coolant boiling must be considered in the framework of SFR safety studies, either locally (in the case of a flow blockage in a single subassembly) or globally

(in the case of a loss of primary flow). Boiling may occur at a large fraction of nominal power (in the case of an unprotected transient) or at residual power (in the case of a protected transient without heat sink).

In past SFR core designs, the rapid removal of coolant resulting from the onset of boiling was associated with a reactivity increase and thus, during an unprotected transient, with a power excursion: hence, in-pile (SLSF [1], SCARABEE [2]) and out-of-pile (KNS37 [3], SIENA [4], GR19 [5]) experiments have mainly studied boiling as an initiating event to a severe accident involving core melting and relocation. More recent designs, such as the CFV core [6], include a liquid sodium plenum above the core. The voiding of this plenum results in a negative reactivity contribution larger than the positive contribution associated with voiding within the core: hence, the onset of boiling will typically result in a power decrease.

In order to study this new phenomenology and assess its consequences in the framework of reactor safety studies, codes capable of representing the thermal-hydraulics of sodium boiling in SFRs must be developed and validated. At CEA, two codes used for SFR single-phase thermal hydraulics have been extended to two-phase studies: the CATHARE system code and the Trio\_U MC core subchannel code. As a system code, CATHARE is capable of predicting the onset of boiling at the scale of a full sub-assembly as well as its consequences on the core neutronics (using a point-kinetics model), within a model of the complete primary circuit; meanwhile, Trio\_U MC can be used to study boiling at a more local level (per-subchannel in the whole core) in order to assess the importance of in-subassembly 3D effects, as well as to perform scaling sensitivity studies for the design of new experiments.

Several physical properties that affect coolant boiling in SFRs differ significantly from those encountered in LWRs. The differences which carry most consequences are the follows:

- the liquid-to-vapor density ratio at operating pressure is much higher (2000, compared to 8 in a PWR): hence, even low-quality boiling is usually associated with high void fractions;
- the thermal conductivity and wettability of liquid sodium are much higher than those of water: hence, a liquid film tends to persist on the core structures until very high void fractions are reached and dry-out occurs by complete evaporation of this film.

For these reasons, any new code developed to study SFR boiling must be validated extensively against sodium experiments representative of the conditions expected during the transient under consideration. In the 1980s, several such experiments were undertaken at CEA, both in-pile and out-of-pile: in particular, the GR19 test series on out-of-pile, SUPERPHENIX-type 19-pin bundles have been chosen for the initial two-phase validation studies of CATHARE and Trio\_U MC codes.

## **2. INTRODUCTION OF GR19 EXPERIMENTS**

GR19 is a 19-pin, electrically-heated test section mounted on the CFNa III CEA loop. This experiment has been built in Grenoble (France) at the end of the 70's and exploited during the 80's. The loop consists in an electromagnetic pump, the main exchanger which provides sodium at 400°C to the test section and the by-pass, a secondary exchanger in the by-pass line, a heater upstream the test section and an expansion vessel where the pressure is maintain at 1.19 bar with argon gaz. The entire loop contains about 150 liter of sodium. Fig.1 is a simplified drawing of the loop.

Four control valves are mounted on the loop so that one can choose the flowrate inside each line. The electromagnetic pump is controlled by the applied voltage [5].

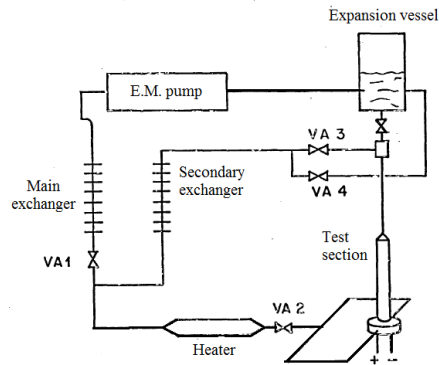


**Figure 1. CFNa III loop (CEA, Grenoble).**

GR19 test section consists in a SUPERPHENIX type 19 pins rod bundle topped with a convergent plenum and a thick tube. Inside the rod bundle, only the middle part (600mm length) is heated. Geometrical data are given for two different test sections (GR19-BP and GR19-I) in Table I.

**Table I. GR19 geometrical data**

<i>(in millimeter)</i>	<b>GR19-BP</b>	<b>GR19-I</b>
<b>Heating length</b>	600	600
<b>Upstream non-heating length</b>	~300	~100
<b>Downstream non-heating length</b>	500	500
<b>Convergent plenum length</b>	170	35
<b>PNS length</b>	866	971
<b>PNS diameter</b>	19.5	19.3
<b>Pin diameter</b>	8.5	8.65
<b>Spacer wire diameter</b>	1.15	1.22
<b>Pin pitch</b>	9.84	9.95
<b>Wire pitch</b>	150	180
<b>Axial flux profile</b>	cosine	uniform

With those two test sections, many phenomenological experiments have been performed: static, quasi-static and Loss Of Flow (LOF) tests. These tests especially aim to investigate stabilized boiling feasibility. Thus, they illustrate stabilized and unstabilized boiling phenomenon whose concept is based on Ledinegg criterion (see §3.2)

### **3. 1-D SIMULATION WITH CATHARE SYSTEM CODE**

#### **3.1. CATHARE System Code Modeling**

CATHARE 2 is a 2-fluid 6-equation thermal-hydraulic code devoted to best estimate calculations of transients in nuclear reactors at system scale. It can also deal with non-condensable gases and radio-chemical components transport.

First designed for Pressurized Water Reactors simulation, it has been extended to SFR applications. The properties of liquid and vapor sodium have been implemented, as well as wall heat transfer coefficients in pure liquid and vapor (see post dry out phase). Quite satisfying results have already been obtained for single phase liquid simulations [7] and the efforts are now reporting on boiling sodium closure laws implementation and validation.

Diphasic thermal models currently used in CATHARE are extracted from water closure laws. Additionally, laws for wall heat transfer from monophasic up to dry out that were applied in the SABENA code (dedicated to Na two phase flow, [8]), have been also implemented to allow sensitivity study along the ongoing qualification process with Na boiling experiments. While thermal aspect may need revision especially regarding flashing delay, condensation and subcooled boiling, wall and interfacial friction laws in CATHARE [9] could be seen at first as applicable since interfacial friction covers bubbly to annular flow and wall friction is based on Lottes-Flinn [10] and Lockart-Matinelli [11], the switch between both being driven by entrainment onset. The former wall friction correlation was indeed used in the SABENA code and the latter was recommended by Na boiling specialists [12]. Additionally, an experimental program was recently carried out at CEA on that topic on a scale 1:1 subassembly mock-up [13] and new interfacial and wall friction correlations have been established in air/water for low quality, high void fraction flows. These developments have been implemented in CATHARE, again to allow sensitivity study along the ongoing qualification process on Na boiling experiments as reported in §4.2 dedicated to internal characteristics.

It has been decided to model the entire CFNa III loop by CATHARE so that inertial phenomena are as accurate as possible and mass flow rate redistribution between the test section and the by-pass - which represents the other assemblies when transposed to the reactor case - can be fully simulated. The test section is represented by a 1-D thermal-hydraulic module with heated and unheated walls, while the expansion vessel is modelled by a 0-D module and Argon gas is defined above the free surface. The main exchanger is modeled by a wall featuring an infinite exchange coefficient with a 400°C boundary. The secondary exchanger however, is not modeled but singular head losses are reported for both. The pump is a simple charge impulse proportional to the tension entered. Fig.2 shows a representation of CATHARE modeling of CFNa III loop with the interface tool GUTHARE (proportions are not respected). The red line marks the heated part of the rod bundle and the blue line the wall which accounts for the main heat exchanger.

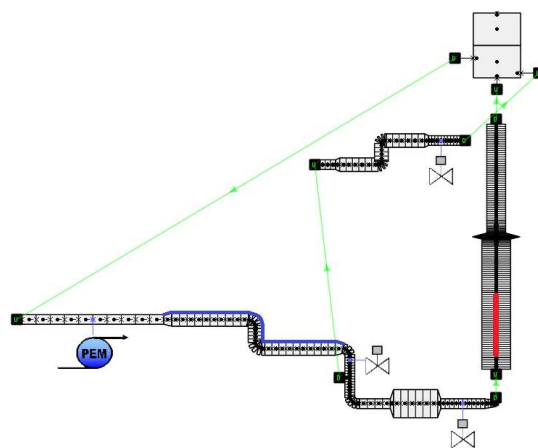


**Figure 2. GUTHARE representation of CFNa III loop.**

### 3.2. Internal Characteristics

When Na boiling starts, due to the high liquid/vapour density ratio, a large amount of void is generated leading to a possible flow blockage of the hydraulic channels [14]. During a loss of flow that is considered for a reactor case hypothetical scenario, this situation can lead to a complete natural circulation interruption and finally to pins dry out prior to severe accident. GR19 tests demonstrated that natural circulation can be achieved or not after a slow loss of forced convection (quasi-static approach) depending on the fulfillment of the hydraulic static criteria established by Ledinegg [15]. Through GR19 tests, the Ledinegg criterion was therefore identified as an efficient approach to predict the possibility of stable boiling for an out of pile slow loss of flow and at least a key parameter to be analyzed for a much more complex reactor case. As described in [14], the definition of the hydraulic Ledinegg criterion is supported by steady state considerations about the internal characteristic (IC) and the external characteristic (EC) of the considered device. The IC is the pressure drop ( $\Delta P$ ) along the channel when the mass flow rate at the inlet is varied under constant power, outlet pressure and inlet temperature. The EC is the driving pressure induced by the external loop as a function of the mass flow rate, this  $\Delta P$  being provided by the pump or the natural circulation. When both characteristics intersect, a hydraulic operating point is defined. The static stability of this working point depends however on the respective slopes of the EC and IC curves. If the condition defined by equation (1) is fulfilled, the working point is indeed stable.

$$\left(\frac{\partial \Delta P_{int}}{\partial Q}\right)_{Q_0} > \left(\frac{\partial \Delta P_{ext}}{\partial Q}\right)_{Q_{0l}} \quad (1)$$

The above discussion highlights the importance of an accurate description of the  $\Delta P$  for a reliable application of the Ledinegg criterion. In that frame, different wall friction models are tested and compared against GR19-BP experimental IC. These models consist in the definition of a two-phase flow multiplier that is applied to the monophasic pressure drop. The latter has been chosen in the rod bundle to be described according to Rheme [16]. The first diphasic multiplier correlation is a combination of Lottes-Flinn (equation (2)) and Lockhart-Martinelli: as mentioned this is the standard modeling of CATHARE for water [9]. The second is Lockhart-Martinelli stand alone (equation (4)) with b and c depending on the liquid and gas flow regimes. The third and last model is the friction law based on the SENSAS experiment [13]: here a corrective coefficient on the two phase friction multiplier of Lottes-Flinn (equation (3)) is proposed. It is worth noticing that the calculated friction depends on the slip between phases: CATHARE uses a 6 equation system where the void fraction depends on the interfacial friction modeling (rod-bundle or pipe laws, see [9]). Although Lockhart-Martinelli is regarded to be a good approach for Na flow [12], its application deserves to be qualified with CATHARE interfacial friction modeling and for a specific low quality flow.

$$\phi_l = \frac{1}{(1 - \alpha)^2} \quad (2)$$

$$\phi_l = \frac{1}{(1 - \alpha)^2} \min [1 ; 1.4429(1 - \alpha)^{0.6492}] \quad (3)$$

$$\phi_l = 1 + \frac{C}{X_{lm}} + \frac{1}{X_{lm}^2}, \quad X_{lm} = \left(\frac{\mu_l}{\mu_g}\right)^{\frac{b}{2}} \left(\frac{1-x}{x}\right)^{\frac{2-b}{2}} \left(\frac{\rho_g}{\rho_l}\right)^{0.5} \quad (4)$$

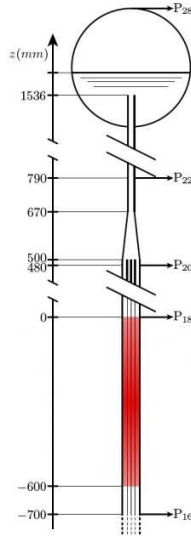


**Figure 3. GR19-BP test bench**

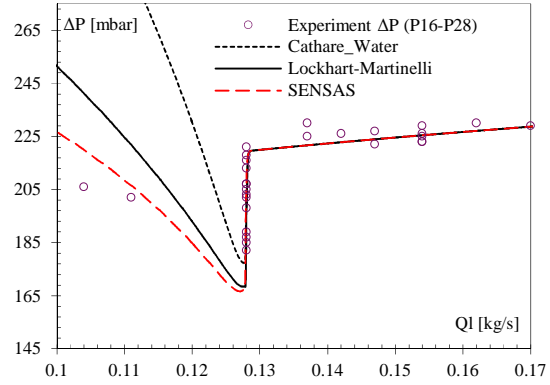


**Figure 4. GR19-BP 5 kw/pin internal characteristic. (P16-P28)**

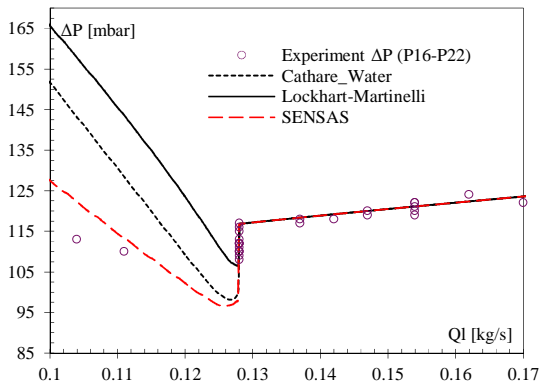


**Figure 5. GR19-BP 5 kw/pin internal characteristic. (P16-P22)**

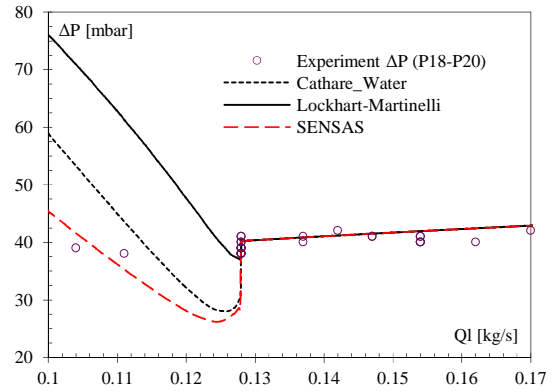


**Figure 6. GR19-BP 5 kw/pin internal characteristic. (P18-P20)**

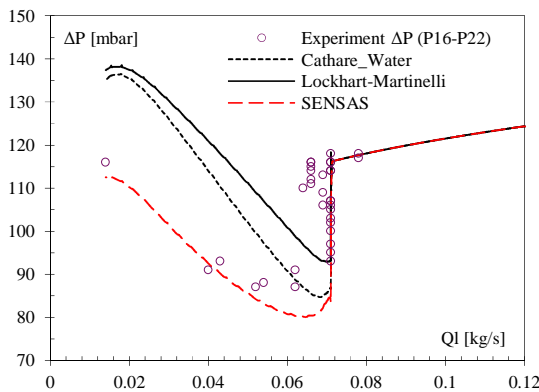


**Figure 7. GR19-BP 3 kw/pin internal characteristic. (P16-P22)**

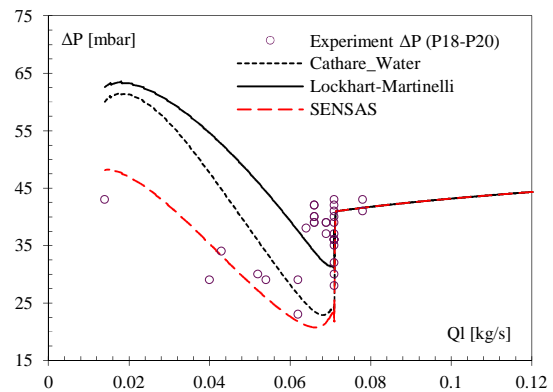


**Figure 8. GR19-BP 3 kw/pin internal characteristic. (P18-P20)**

Fig.4 to 8 feature a characteristic “S” shape: just after boiling onset there is an initial gravitational pressure drop; when the Na mass flow further decreases, the boiling front advances within the pin bundle and the effect of the two phase friction is unveiled.

Within the rod bundle (Fig.5 and Fig.7) Lockhart-Martinelli friction provides more  $\Delta P$  compared to the standard CATHARE water correlation, being this behavior the inverse in the outlet piping region to the point of inverting the total  $\Delta P$  between models. Hence if the total  $\Delta P$  is monitored (Fig.4), Lockhart-Martinelli relaxes the overall pressure drop compared to the CATHARE water model. Between these locations (pipe and rod bundle) the interfacial friction modeling is different, the void accumulates in the outlet tube being the low gas quality CATHARE water model (Lottes-Flinn) more sensible to it due to its void fraction dependance. For these conditions the friction developed for SENSAS relaxes the overall pressure drop in good agreement with the experimental data even for high gas quality flow (Fig.7 and Fig.8), conditions that are beyond the scope of establishment of the SENSAS model. Nevertheless further studies are needed to assess the behave of the model at high gas qualities especially in the outlet pipe. Currently the 37 pins ECONA test bench experimental data [17] is being used for additional friction modeling qualification.

### 3.3. Flow Redistribution or stable boiling with a Quasi-static Approach

This paragraph presents results obtained with CATHARE code on very slow LOF transients in the loop with GR19-I test section. During each test, inlet temperature, outlet pressure and power stay constant but the flow rate is cut step by step decreasing pump voltage and closing the inlet valve. Thus, it is a quasi-static approach to boiling phenomena.

For low power tests (such as 3kW/pin test), stable boiling is achieved. No mass flow rate experimental data are available to compare to CATHARE prediction. Nevertheless, CATHARE has proved be able to reproduce boiling stability.

For higher power tests (such as 8kW/pin test), the Ledinegg criteria is not respected so it can be expected boiling to be unstable. Indeed, the test shows that boiling leads to a strong decrease of mass flow rate in the test section: this phenomenon is named flow redistribution. The time between boiling onset and zero mass flow rate is high enough to be noticed: in this case, it lies between 40 and 50 seconds. The exact experimental redistribution time is unknown since pins power was cut off before reaching zero mass flow rate. Indeed, from this point, dry out can appear very quickly and any risk of pins damage had to be avoided. Comparison of inlet mass flow rate simulation with experimental data is given Fig.9.

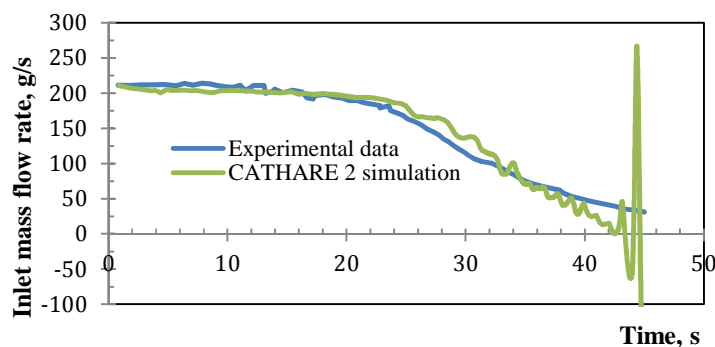


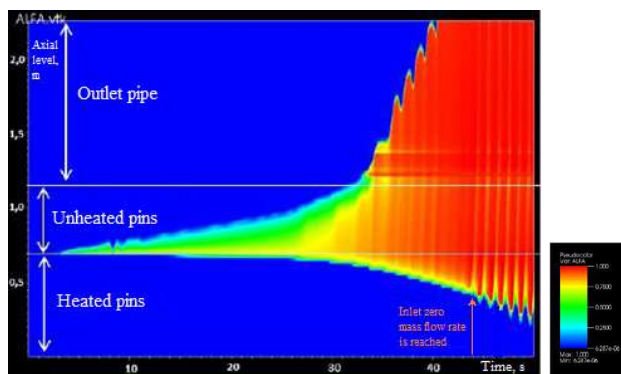
**Figure 9. Comparison between CATHARE simulation (in green) and experiment (in blue) for quasi-static loss of flow experiment with 8kW/pin GR19-I.**



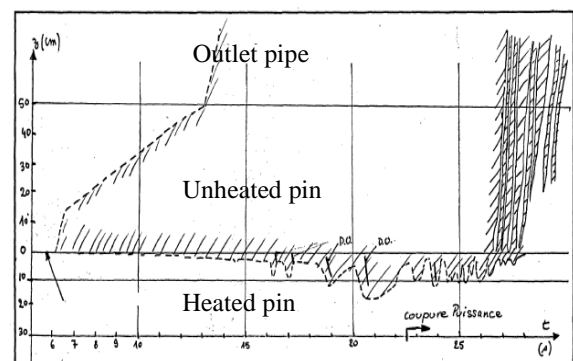
One can see on Fig.9 a quite good match between simulation and experiment. Simulation follows the experimental trend and gives several tens of seconds which is quite encouraging. However, one has to stay critical on these results. Uncertainties remain on physical models used on CATHARE for sodium boiling application.

Fig.10 is taken from CATHARE simulation and shows void fraction progression inside the test section. The color gives the amount of void fraction (red is for large vapor fraction). The abscissa is time and the ordinate is axial level in the test section. It can be seen that boiling starts at the end of the heated part of the rod bundle, and spreads first faster downstream (unheated bundle) than upstream (heated bundle). When it reaches the outlet pipe, the boiling front progression is significantly increased in both directions. The corresponding experimental void fraction map is not available however the calculated phenomenology is consistent with the one that was monitored along another slow redistribution test performed with a single pin, which is reported on Fig.11. This latter experiment performed on the CESAR loop had consisted in increasing the initial 9.4 kW pin power of 20%, while the initial outlet Na temperature was already close to boiling onset (885°C).

When inlet mass flow rate reaches zero, about 40% of the heated pins length is taken by boiling sodium, which is not so far from what is found in the experiment (one third). Moreover, from that point, one can see some oscillations which can stand for temporary dry out.



**Figure 10. boiling front progression (axial position vs time) simulated by CATHARE code.**



**Figure 11. boiling front progression (axial position vs time) monitored on the CESAR loop during the TR8 test.**

### 3.4. Instantaneous LOF Experiments

GR19 tests were the opportunity for experimenters to investigate Ledinegg criteria applicability for fast loss of flow transient. They found out that one can achieve stable boiling during fast LOF transient but for lower pin power than for quasi-static transient. When 5kW/pin was still able to achieve stable boiling according to Ledinegg criteria, it came out that it led to flow redistribution if the pump was cut off instantaneously. 3kW/pin however, always leads to stable boiling.

CATHARE has shown its ability to reproduce these specificities at 3kW/pin and 5kW/pin with fast LOF transient. Fig.12 is the comparison of the inlet mass flow rate calculated by CATHARE code with the one given by the inlet flowmeter for the 3kW/pin LOF experiment. One can observe the good trend of the simulation compared to the experiment. The time to come back to boiling stability is well reproduced. However the minimal calculated mass flow rate is much higher than experimental one and stabilization is reached a little lower. Moreover, it seems CATHARE doesn't succeed in reproducing experimental

dynamic instabilities during mass flow rate climb up (chugging at boiling onset). This could be explained by the fact that the minimum mass flow rate is not reached or because head losses in the loop and heat losses in the test section are not well reproduced (some data are not available). Indeed, in case the effective amount of boiling in the test section is strengthened by closing VA1 valve or reducing heat losses, dynamic instabilities are obtained, even in the stable boiling part, whose physical or numerical nature is still to be defined. Thus, studies keep going on and CATHARE models are checked, especially thermal closure laws.

As for the 5kW/pin LOF experiment, Fig.13 compares calculated inlet mass flow rate with measured one. As one can see on the experimental plot, very strong dynamic instabilities appear. Boiling does not succeed in stabilizing and flow redistribution occurs. Simulation displays as well this unstable characteristic but it does not reproduce the redistribution time neither the dynamic instabilities. As for previous case, this could be due to the fact that CATHARE begins the transient with a higher mass flow rate. Investigations continue but one has to keep in mind that these tests present harder conditions than the ones which could be found in the reactor case where mass flow rate drop during an ULOF transient is more progressive. Anyway, CATHARE models should be revised to better trace out thermal hydraulic dynamic.

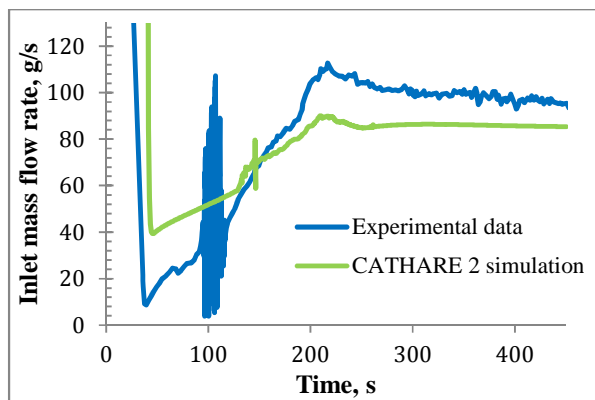


**Figure 12. Comparison between CATHARE simulation (in green) and experiment (in blue) for fast loss of flow 3kW/pin experiment.**

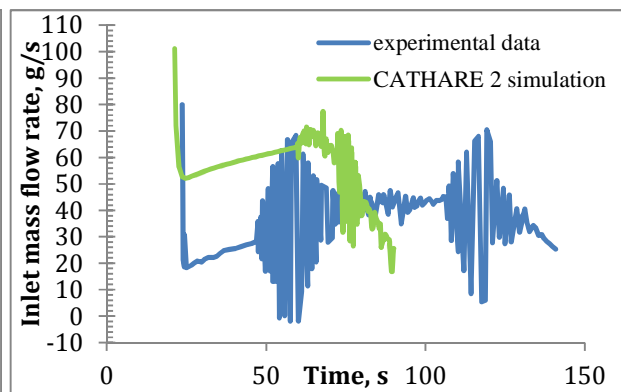


**Figure 13. Comparison between CATHARE simulation (in green) and experiment (in blue) for fast loss of flow 5kW/pin experiment.**

### 3.5. Outcomes and perspectives for the code

The outcomes of this study with GR19 experiments are the follows:

- Static tests provided the information that CATHARE calculated too high wall frictions. A first revision of the models has been carried out to overcome it, based on the use of the Lockart-Martinelli correlation from boiling onset. Complementary work is under progress on other Na boiling experiments to further balance the relevancy of the SENSAS correlation for Na boiling at low flow quality.
- Dynamic tests showed that CATHARE is able to achieve reasonable agreement compared to the available data. So, at the moment, there is no reason to disregard reactor case results. However, matching still can be improved. That is why, closure laws modification will be considered, in particular regarding thermal aspect (flashing, condensation, etc...). The presented work will then have to be revised and new tests will have to be simulated as well, to balance the set of closure laws. Numeric of the code has also to be strengthened.

## 4. 3-D SIMULATION WITH MC SUBCHANNEL CODE

### 4.1. The Trio\_U MC code

SFR core design studies require a finer knowledge of core thermal hydraulics than those accessible from a 1D description of each subassembly (S/A), in particular in order to determine the maximum cladding temperature across the core in its nominal state. Because of the high computational cost of modeling even a single subassembly in CFD, these design calculations are typically performed at the coarsest scale capable of determining the per-pin cladding temperature: the subchannel scale, with one radial mesh per sodium interstice between the fuel pins (Fig.14).

At CEA, SFR subchannel codes were developed in the 1970s and 1980s for the design studies of PHENIX and SUPERPHENIX. In 2008, these codes were improved and integrated into a modern CFD code, Trio\_U, in the framework of ASTRID design studies. The resulting code, Trio\_U MC, can perform subchannel calculations of a complete SFR core (Fig.14): it can also be coupled to a Trio\_U CFD model of the hot-plenum and the inter-wrapper region in order to determine the effect of sodium flows between the subassemblies' hexagonal wrappers.

At the subchannel scale, fine geometrical details, such as the helical wire-wrappers around each fuel pin, cannot be represented: hence, correlations must be introduced to account for their large-scale effects. The main correlations used in Trio\_U MC are the Cheng-Todreas detailed correlation for the local pressure drop and for the wire-wrapper mixing effects [18].

The initial design goal of Trio\_U MC was to perform whole-core steady-state calculation of thermal hydraulic fields for design studies. Hence, the code initially adopted a fast, "marching-type" resolution method: by neglecting transverse pressure gradient within each rod-bundle, this method can compute forced or mixed-convection steady states in very short times (around 30s on 1 CPU for a complete core).

In order to extend the code to the computation of transients and to natural convection cases, a staggered-grid, semi-implicit numerical method was added to the code in 2014. Known as MC-T ("transient"), this method is much more computationally expensive than its steady-state counterpart, but is still capable of computing complete-core transients in a reasonable time (around 3 hours on 50 CPUs for a LOF transient), thanks in large part to parallelization efforts.

### 4.2. Two-phase developments

The phenomenology of sodium boiling in a subassembly includes a number of 3D effects that remain inaccessible to a one-dimensional model such as used in CATHARE:

1. in a steady-state, the temperature gradient between the center and the peripheral subchannels of an S/A may lead to a boiling region limited to the center of the S/A (local boiling);
2. during a transient such as a quasi-static flow redistribution (Fig.9) or a faster loss-of-flow scenario, the same gradient will cause the boiling front to propagate faster in the center of the bundle than in its periphery: the resulting heterogeneous progression will be hard to predict from a 1D approach.

In addition, these effects are expected to have a higher influence in smaller bundles ( $\leq 37$  pins), such as those used in out-of-pile experiments, than in the large bundles corresponding to reactor cases ( $\geq 217$  pins). A 3D approach thus seems to be necessary in order to evaluate the representativity of existing smaller-scale experiments to reactor conditions, as well as to guide the design of future experiments.

To that end, the following developments were undertaken in Trio\_U MC:

1. in 2013, the code's initial steady-state resolution method was extended with a simplified, 4-equations boiling model used in the BACCHUS code [19]. This model postulates kinematic equilibrium (the absence of slip between liquid and vapor), but allows for a departure from thermodynamic equilibrium : the flow quality  $x$  relaxes towards its equilibrium value  $x^*$  through an equation of the form

$$\frac{Dx}{Dt} = \frac{x^* - x}{\theta},$$

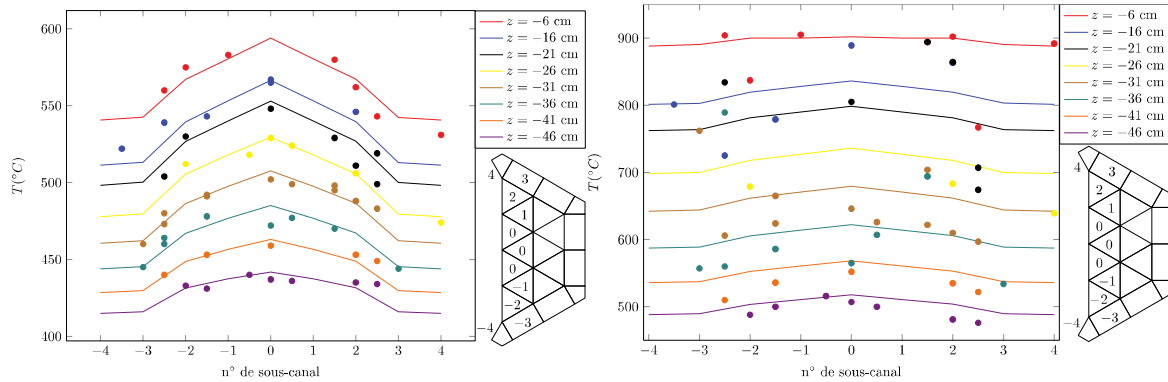
where the relaxation time  $\theta \approx 10 \text{ ms}$  accounts for the latency between the heating of the liquid and its boiling. Because of the assumption of kinematic equilibrium, this model is considered adequate only in boiling cases with low quality (such as local boiling). The resulting code version is designated MC-Eb ("boiling");

2. in 2015, the MC-T transient, semi-implicit resolution was extended to a two-fluid, six-equations model similar to those used in CATHARE. Two-fluid models rely on a number of physical correlations in order to describe the mass, momentum and energy exchanges between the phases and with the structures surrounding the fluid: initially, the correlations used in the SABENA code [20] were considered. In the following, the resulting version is designated MC-TEb ("transient boiling").

It should be noted that, by design, Trio\_U MC is not capable of modeling a complete experimental loop. In cases where loop effects are important (such as a reactor case or a flow redistribution transient), a code coupling of a MC model of the S/A with a CATHARE model of the complete loop is under consideration.

#### 4.3. Validation of MC-Eb and MC-TEb on GR19-BP

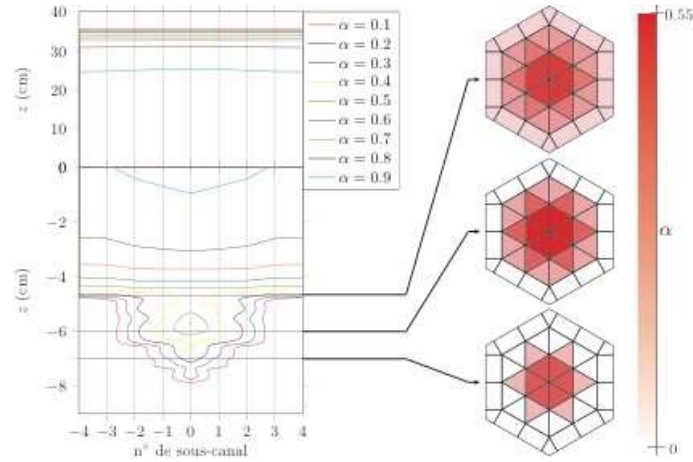
Preliminary validation of the two-phase predictions of Trio\_U MC has been carried out on the GR19-BP experiment (see §2). In particular, the ability of MC-Eb (steady-state, simplified boiling model) to predict the extent of local boiling was tested on experimental steady-states performed at 5 KW / pin.



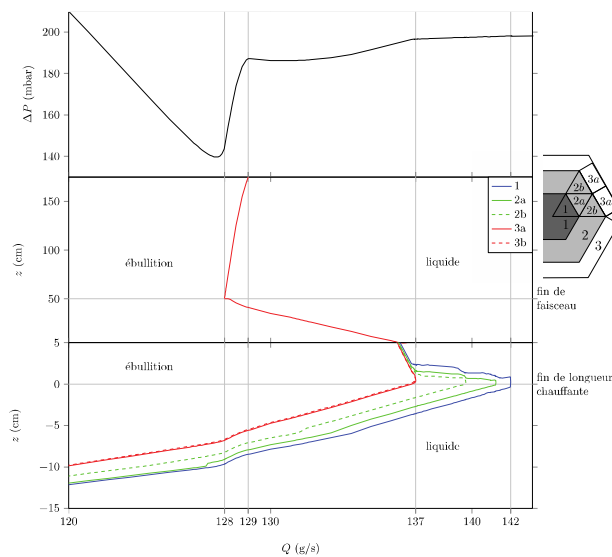
**Figure 14. Experimental measurements (dots) and MC-Eb predictions (lines) for in-bundle temperatures predicted in GR19-BP at 5KW/pin, for  $Q = 0.4 \text{ kg/s}$  (left) and  $Q = 0.13 \text{ kg/s}$  (right). Heights are relative to the top of the heated length ( $z = 0$ ).**

Fig.14 presents code-to-experiment comparison of in-bundle temperatures for a single-phase case (left) and a boiling case (right). The first case confirms the code's ability to correctly predict the temperature distribution within the bundle. In the second case, a systematic overestimation of the bundle temperatures at  $-40 < z < -15 \text{ cm}$  can be observed: this effect is introduced by the increasing resistivity of the bundle's heating elements with increasing temperatures (which skews the axial power profile), but does not affect the total power (and thus the temperatures at the top of the heated length). The onset of boiling

results in a flattening of the temperature profile at  $T \approx T_{sat}$  (around 900°C here): the extent of the boiling region calculated by the code in this case is shown in Fig.15.



**Figure 15. Extension of the boiling region relative to the top of the heated length ( $z = 0$ ) in GR19-BP at 5KW / pin power and  $Q = 0.13$  kg/s**



**Figure 16. Onset and generalization of boiling in GR19-BP at 5KW/pin with decreasing flow : radial propagation of the boiling region (bottom) and overall pressure drop (top)**

Figure 16 shows the influence of the 3D extension of the boiling region on the bundle internal characteristic (above):

- local boiling occurs at  $137 < Q < 142$  g/s, with no influence on the overall pressure drop;
- boiling becomes generalized and propagates upwards in the bundle at  $129 < Q < 137$  g/s;
- around  $Q = 129$  g/s, boiling exits the bundle, inducing the S-curve drop in the internal characteristic;
- below  $Q = 128$  g/s, the increasing void fraction results in a pressure drop increase.

The two-phase pressure drop increase at low flow is over predicted by MC-Eb, because the simplified boiling model used in the code neglects slip between the two phases, as shown in Fig.17. Preliminary results obtained with MC-TEb using the SENSAS correlation (3) show that the two-fluid model used in that version results in an improved prediction in this case.

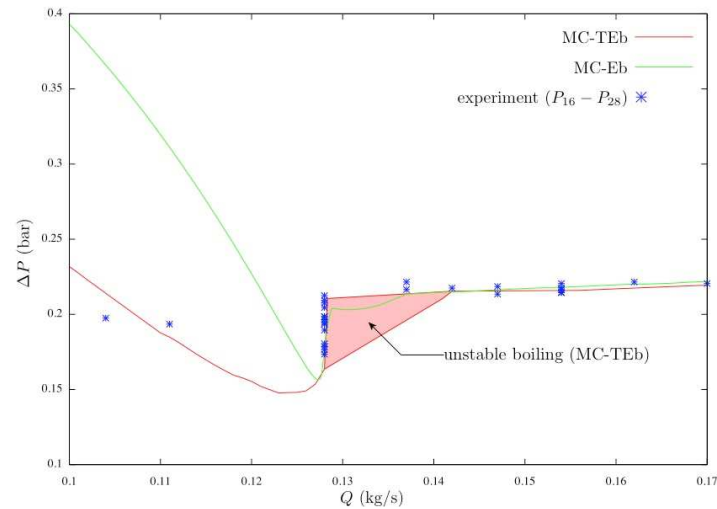


**Figure 17. Predictions of the GR19BP total internal characteristic (P16 - P28) at 5KW/pin by MC-Eb and MC-TEb. Between  $0.13 < Q < 0.14$  kg/s, MC-TEb predicts unsteady boiling with periodic oscillations.**

## 5. CONCLUSIONS

To support CEA R&D program on Generation IV SFR, thermal hydraulic codes are developed and validated, including in boiling sodium field. In particular, the CEA reference CATHARE system code and Trio\_U MC subchannel code are currently under evaluation and improvement. To that end, the GR19 out-of-pile experiment at CEA has been selected to first evaluate the codes' performances and to guide future code developments.

In this paper, main GR19 features and tests are described. Simulation results on these tests with both codes are given. Their good performances and limits are highlighted: the CATHARE code achieved reasonable agreement compared to the available data in particular for quasi-static experiments, and it proved its ability to reproduce stable boiling phenomena. However, its predictions can still be improved by modifying closure laws, especially regarding energy exchanges. Meanwhile, the Trio\_U MC code showed its ability to predict correctly the occurrence and extension of steady-state local boiling; however, further improvements will be needed to correctly model unstable and transient boiling where the slip between phases has to be taken into account. These developments will be undertaken in the new version of the code: MC-TEb.

For some reactor transients, such as those which lead to low natural convection, coupling between those two codes could be required. At that time, each code should be validated separately. Then, it will be necessary to validate coupling methods as well.

## REFERENCES

- [1] J. Henderson, S. Wood and R. Rothrock, "HEDL W-1 SLSF experiment LOPI transient and boiling test results," in *HEDL-SA-FP-2012, American Nuclear Society annual meeting, Las Vegas, NV, USA, 8 Jun, 1980*.
- [2] M. Livolant, "SCARABEE : a test reactor and programme to study fuel melting and propagation in connexion with local fault. Objectives and results", in *International Fast Reactor Safety Meeting, Snowbird, USA, 1990*.
- [3] S. Gonzalez, "Development of a 37-pin bundle with a sinusoidal axial power distribution for LOF simulation tests," in *8th meeting of the liquid metal boiling working group, 1978*.
- [4] K. Haga, "Sodium Boiling Experiment in a 37-Pin Bundle under Loss-of-Flow Conditions," in *10th meeting of the liquid metal boiling working group, 1982*.
- [5] B. Rameau, "Out of pile contribution to the study of sodium boiling under forced and mixed convection in a cluster geometry –GR19 I experimental results and analysis.," in *10th Liquid Metal Boiling Working Group Karlsruhe, Germany, October 27–29, 1982*.
- [6] F. Varaine, "Pre-conceptual design study of ASTRID core," in *Proceedings of ICAPP 2012, Chicago, USA, June 24-28, Paper 432757, 2012*.
- [7] D. Tenchine, "Status of CATHARE code for sodium cooled fast reactors," in *Nuclear Engineering and Design, 245, pp. 140-152, 2012*.
- [8] H. Ninokata, "Six equation two phase flow model code SABENA for sodium boiling simulation.," in *Grenoble, 11th meeting of the liquid metal boiling working group, 1991*.
- [9] D. Bestion, "The physical closure laws in the CATHARE code," *Nuclear Engineering and Design*, vol. 124, no. 3, pp. 229-245, 1990.
- [10] P. Lottes and W. Flinn, "A method of analysis of natural circulation boiling systems," in *Nucl. Sci. Eng., vol. 1, p. 420, 1956*.
- [11] R. Lockhart and R. Martinelli, "Proposed correlation of data for isothermal two phase, two component flow in pipes," *Chemical Engineering progress*, vol. 45, 1949.
- [12] H. M. Kottowski, *Liquid metal thermal hydraulics*, Freiburg: Inforum Verlag, 1994.
- [13] J. Perez, N. Alpy, D. Juhel and D. Bestion, "CATHARE 2 simulations of steady state air/water tests performed in a 1:1 scale SFR sub-assembly mock-up," *Annals of nuclear Energy (article in Press)*, 2015.
- [14] J. M. Seiler, D. Juhel and P. Dufour, "Sodium boiling stabilisation in a fast breeder subassembly during an unprotected loss of flow accident," *Nuclear Engineering and Design*, vol. 240, p. 3329–3335, 2010.
- [15] J. Boure, "Review of two-phase instability," in *ASME-AICHE Heat Transfer Conference, Tulsa, 1971*.
- [16] K. Rehme, "Pressure drop correlations for fuel element spacers," *Nuclear Technology*, vol. 17, no. 1, p. 1973, 1973.
- [17] B. Rameau and N. Bourabaa, "Sodium boiling natural convection tests in a 37 pin bundle. ECONA experiment," 13th meeting of the liquid metal boiling working group, Winfrith, 1988.
- [18] S. Cheng and N. Todreas, "Hydrodynamic models and correlations for bare and wire-wrapped hexagonal rod bundles—bundle friction factors, sub-channel friction factors and mixing parameters," in *Nuclear Engineering and Design 92, 227–251, 1986*.
- [19] G. Basque, D. Grand and B. Menant, "Theoretical analysis and experimental evidence of three types of thermohydraulic incoherency in undisturbed cluster geometry," in *8th meeting of the liquid metal boiling working group, 1978*.
- [20] H. Ninokata, "SABENA: subassembly boiling evolution numerical," *Nuclear Engineering and Design 120 (1990) 349-367, 1990*.